European Journal of Pharmaceutics and Biopharmaceutics 70 (2008) 735–740

Contents lists available at ScienceDirect

European Journal of Pharmaceutics and Biopharmaceutics

journal homepage: www.elsevier.com/locate/ejpb

Research paper

Preparation of estradiol chitosan nanoparticles for improving nasal absorption and brain targeting

Xiaomei Wang, Na Chi, Xing Tang *

Department of Pharmaceutics, Shenyang Pharmaceutical University, Shenyang, China

ARTICLE INFO

Article history:
Received 2 January 2008
Accepted in revised form 5 July 2008
Available online 18 July 2008

Keywords:
Estradiol
Chitosan nanoparticles
Nasal delivery
Pharmacokinetics
Microdialysis
Brain targeting

ABSTRACT

The estradiol(E_2)-loaded chitosan nanoparticles (CS-NPs) were prepared by ionic gelation of chitosan with tripolyphosphate anions (TPP). The CS-NPs had a mean size of (269.3 ± 31.6) nm, a zeta potential of +25.4 mV, and loading capacity of E_2 CS-NPs suspension was 1.9 mg ml^{-1}, entrapment efficiency was 64.7% on average. Subsequently, this paper investigated the levels of E_2 in blood and the cerebrospinal fluid (CSF) in rats following intranasal administration of E_2 CS-NPs. E_2-loaded CS-NPs were administered to male Wister rats either intranasally or intravenously at the dose of 0.48 mg kg^{-1}. The plasma levels achieved following intranasal administration (32.7 ± 10.1 ng ml^{-1}; t_{max} 28 ± 4.5 min) were significantly lower than those after intravenous administration (151.4 ± 28.2 ng ml^{-1}), while CSF concentrations achieved after intranasal administration (76.4 ± 14.0 ng ml^{-1}; t_{max} 28 ± 17.9 min) were significantly higher than those after intravenous administration (29.5 ± 7.4 ng ml^{-1} t_{max} 60 min). The drug targeting index (DTI) of nasal route was 3.2, percent of drug targeting (DTP%) was 68.4%. These results showed that the E_2 must be directly transported from the nasal cavity into the CSF in rats. Finally, compared with E_2 inclusion complex, CS-NPs improved significantly E_2 being transported into central nervous system (CNS).

1. Introduction

Alzheimer's disease (AD), the most common cause of dementia, affects millions of people over the age of 65 in the Western world and an increase in the occurrence of AD is expected in the future, as the proportion of older people in the population grows. AD is a chronic neurodegenerative disorder accompanied by the gradual and progressive loss of functional and psychomotor abilities [1].

There has been speculation that a person's sex could be a risk factor for AD, 17β-estradiol concentrations in women with AD have been reported to be decreased in comparison with healthy controls. 17β-Estradiol, the most potent female sex hormone, belongs to the family of steroid hormones. Apart from its influence on primary and secondary sexual characteristics, it is also involved in the regulation of brain development. Long-term oestrogen replacement has proved to be beneficial in the prevention and treatment of Alzheimer's disease [2–4].

In the recent years, the nasal route has received a great deal of attention as a convenient and reliable method for the systemic administration of drugs. Nasal delivery has been explored as an alternative administration route to target drugs directly to the brain via the olfactory neurons [5–8] providing more opportunities for estradiol to enter the central nervous system (CNS) and then treat Alzheimer's disease. Therefore, how to improve the amount of drug transported into CNS becomes the focus of attention.

Nasal mucociliary clearance is one of the most important limiting factors for nasal drug delivery. It severely limits the time allowed for drug absorption to occur and effectively rules out sustained nasal drug administration. However, bioadhesive polymers can be used to increase the nasal residence time, thus allowing longer absorption times, and to achieve a more intimate contact with the nasal mucosa, which results in a higher concentration gradient and subsequent increased absorption [9].

Another important limiting factor in the nasal application is the low permeability of the nasal mucosa for the drugs. It seems to be necessary to consider an absorption enhancement mechanism for co-administration of drugs with either mucoadhesive polymers or penetration enhancers or combination of the two [10–12].

Chitosan, a cationic polysaccharidc, is commercially available in a range of grades with different molecular weights and degrees of deacetylation. Industrially, they are produced from chitin (the schemes of chitin and chitosan are shown in Fig. 1), the world's second most abundant biopolymer, by a deacetylation process involving alkaline hydrolysis. The term chitosan refers to a family

* Corresponding author. Department of Pharmaceutics, Shenyang Pharmaceutical University, No. 103, Wenhua Road, Shenyang, China. Tel.: +86 24 23986343; fax: +86 24 23911736.
E-mail address: tangpharm@yahoo.com.cn (X. Tang).

0939-6411/$ - see front matter © 2008 Elsevier B.V. All rights reserved.
doi:10.1016/j.ejpb.2008.07.005

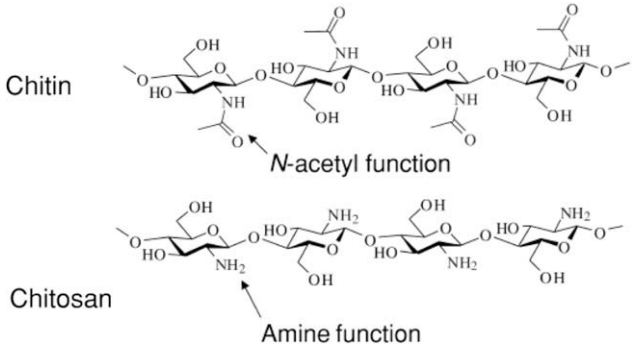

Fig. 1. Chitin and chitosan.

of polymers, individually characterized by their ratio of acetylated to deacetylated units and molecular weight, both parameters being equally responsible for the properties of the polymer.

Chitosan has been used for a range of applications as diverse as for water purification, as a food ingredient and as a pharmaceutical excipient in oral drug formulations for the improvement of the dissolution of poorly soluble drugs or to obtain controlled drug release [13,14]. It has previously been shown that chitosan has a great potential as a nasal delivery system, facilitating the passage of large hydrophilic molecules such as salmon calcitonin and insulin, through the nasal mucosa and into the systemic circulation [15]. However, the clinical use of chitosan in nasal preparations necessitates the evaluation of their effect on the nasal epithelium and the mucociliary clearance system.

On the basis of our former study [16], we prepared estradiol chitosan nanoparticles, aiming at reducing nasal mucociliary clearance and enhancing permeation of E_2 into the nasal mucosa, and then improving the E_2 bioavailability, especially for brain targeting.

2. Materials and methods

2.1. Materials

Estradiol (17β-estradiol) was purchased from Xianju Pharmaceutical Factory, China. Randomly methylated β-cyclodextrin (RAMEB) was obtained from Wacker-Chemie, Germany. Chitosan (deacetylation degree 95.0%, molecular weight 50,000) was provided by Zhejiang Yuhuan marine biochemistry Ltd., China. Sodium tripolyphosphate (TPP) was given from Shenyang Dongxing Reagent Factory, China. All other reagents were of analytical grade or the highest grade commercially available.

Microdialysis probes were U-shaped and made of hollow cellulose fiber (DM-22, 200 μm inner diameter and 220 μm outer diameter, EICOM CORP, Japan). The membrane was 4 mm in length with a molecular weight cut-off of 5000 Da. Artificial CSF composed of 128 mM NaCl, 2.6 mM KCl, 1.26 mM $CaCl_2$ and 2 mM $MgCl_2$ was prepared using deionized distilled water. The solution was filtered through a 0.22 μm nylon filter before use.

Male Wister rats weighing 250–300 g were provided by the animal house of Shenyang Pharmaceutical University, China. These animals were allowed to acclimatize in environmentally controlled quarters (24 ± 1 °C and 12:12 h light–dark cycle) for at least 5 days before being used for experiments.

2.2. Preparation of E_2 chitosan nanoparticles (CS-NPs)

E_2-loaded chitosan nanoparticles were prepared by ionic interaction. A 0.2% w/v solution of chitosan was prepared in 1% v/v acetic acid solution. TPP (0.1% w/v) was dissolved in purified water, while E_2 inclusion complex [16] was dissolved in CS acetic acid solution to ensure the concentration of E_2 in the final CS-NPs suspension reaching 2 mg ml^{-1}.

The chitosan solution (5.0 ml) was stirred at 1500 rpm with a DF-101S magnetic stirrer (Gongyi Yuhua Instrument Co., Ltd., China) at room temperature (25 °C). The TPP solution (2.0 ml) was gently added to the system through a No. 4 syringe needle at the speed of 2 ml h^{-1}, and nanoparticles were formed, stirring for 30 min. Subsequently, a certain amount of 1 N HCl or NaOH solution was added to adjust the pH of the suspension to pH 5.

2.3. Physicochemical characterization of E_2 CS-NPs

The particle size and zeta potential were measured using a NICOMPTM 380 Zeta Potential/Particle Sizer (Particle Sizing Systems, Santa Barbara, USA). The mean particle size and distribution were measured based on photon correlation spectroscopy (PCS, dynamic light scattering, DLS) technique, which is a powerful and versatile tool for estimating the particle size distribution of fine-particle materials ranging from a few nanometers to several micrometers [17]. The zeta potential is a very useful way of evaluating the stability of any colloidal system, and it was determined based on an electrophoretic light scattering (ELS) technique.

2.4. High-performance liquid chromatographic analysis in vitro [18]

The HPLC equipment consisted of a HITACHI L-7110 Intelligent HPLC pump, and a HITACHI L-7200 Intelligent HPLC Autosampler, a HITACHI L-7420 Intelligent HPLC Detector, and a ANASTAR Chromatography Data System. Separation was achieved under room temperature on a Kromasil C_{18} column (200 mm × 4.6 mm, particle size 5 μm, Zirchrom company). The mobile phase consisted of acetonitrile–water (50:50, v/v%), filtered and degassed under reduced pressure, prior to use. The flow rate was 1.0 ml min^{-1} and peak detection was performed at 205 nm. The injection volume was 20 μl.

2.5. Evaluation of E_2 loading capacity and entrapment efficiency

For determining E_2 loading capacity, the Stand solution (about 10 μg ml^{-1}) was prepared by dissolving E_2 in methanol, and the Test solution was obtained as follows: 0.5 ml CS-NPs suspension of the three batches was shifted into a 50 ml volumetric flask, and then diluted with 1% (v/v) acetic acid solution, being ultrasound damaged for 30 min, finally, filtrated through 0.22 μm microporous membrane.

The entrapment efficiency of the process was determined upon separation of nanoparticles from the aqueous suspension containing non-entrapped E_2 by ultra centrifugation at 40,000 r min^{-1}, 10 °C for 30 min. The amount of free E_2 in the supernatant was measured by HPLC. E_2 entrapment efficiency (EE%) and loading efficiency (LC) in the CS-NPs were calculated according to the equations below:

$$EE\% = \frac{\text{Total amount of } E_2 \text{ loading} - \text{free } E_2 \text{ in the supernatant}}{\text{Total amount of } E_2 \text{ loading}} \times 100 \quad (1)$$

$$LC(\text{mg ml}^{-1}) = \frac{\text{Total } E_2 \text{ amount} - \text{free } E_2 \text{ amount}}{\text{Suspension volume}} \quad (2)$$

2.6. Animal experiments

2.6.1. Nasal cavity isolation and jugular vein cannulation

The rats were anesthetized with an intraperitoneal injection of urethane (1.2 g kg^{-1}). During the experiment, body temperature was maintained at 37 °C under an infrared lamp. The nasal cavity was isolated from the respiratory and gastrointestinal tracts using a procedure described by Hirai et al. [19] and Huang et al. [20].

Briefly, after an incision was made in the neck, the trachea was cannulated with a polyethylene tube to maintain respiration. Another PE-200 tube was inserted through the esophagus toward the posterior part of the nasal cavity and ligated. The passage of the nasopalatine tract was sealed with an adhesive agent to prevent the drainage of the solution from the nasal cavity to the mouth. A polyethylene tube was inserted into the jugular vein for blood sampling.

2.6.2. Microdialysis probe implantation into rat brain

The rats had their skulls shaved and were placed in a stereotaxic apparatus after being anesthetized. A midline incision of approximately 2 cm was made parallel to the sagittal suture. The bregma was located and used as the reference point for positioning the microdialysis probe. A microdialysis probe was stereotaxically inserted through a cranial burr hole made by a dental drill to a depth of 3.1 mm, using the following coordinates, in relation to the bregma: 1.5 mm lateral, 0.9 posterior, and the probe was attached to the skull with dental cement.

2.6.3. E_2 CS-NPs administration and collection of biological samples

For intranasal administration, the E_2 CS-NPs suspension (2.0 mg kg^{-1}) was instilled into the right nostril at a dose of 0.48 mg kg^{-1} via a microsyringe, which was attached to a blunt needle. Blood samples (0.3 ml) were drawn from the tube in the jugular vein into heparin stabilized test-tubes at different times: 0, 5, 10, 20, 30, 45, 60, 90, 120, 150, and 180 min. After each blood withdrawal, the same volume of sterile normal saline was put back into the circulation to maintain the total blood volume. CSF perfusate samples were collected at the intervals of 20 min for 240 min. Plasma was separated by centrifugation at 3000 rpm for 15 min and kept frozen at −20 °C together with CSF perfusate for subsequent analysis.

Intravenous administration was carried out by injecting a dose of 0.48 mg kg^{-1} E_2 CS-NPs suspension (0.2 mg ml^{-1}) via the femoral vein. The method of sample collection was the same as above.

Both nasal and intravenous administration should be performed following the successful implantation of a microdialysis probe and stabilization for 1 h with artificial CSF.

2.6.4. Microdialysis procedure

The inflow to the microdialysis probe was driven by a microinjection pump (S200, KD Scientific Company, USA), perfused with artificial CSF, and the outflow was collected in small polypropylene tubes. Before and during the implantation procedure the probe was filled with artificial CSF solution at a rate of 10 μl min^{-1}. Then, 5 min after implantation of the probe, the flow rate was reduced to 4 μl min^{-1} and was maintained at this level throughout the experiment. The microdialysis experimental device is shown in Fig. 2.

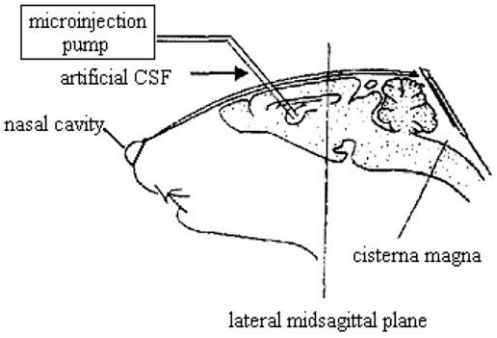

Fig. 2. The perfusion of artificial CSF to the lateral ventricle and collection of the CSF sample from it.

2.6.5. Analytical method

2.6.5.1. Disposition of biological samples. Briefly, 0.1 ml plasma was spiked with 5 μl internal standard (ethyl hydroxybenzoate, 12.5 μg ml^{-1}) solution. The sample was then vortexed with ether (5 ml) for 5 min, and centrifuged for 5 min at 3000gmin^{-1} before the supernatant was transferred to a new glass tube and evaporated to dryness in a water bath at 40 °C under N_2 flow. The residue was dissolved in 200 μl methanol, then 50 μl was injected onto the HPLC column.

CSF perfusate samples were injected directly into the HPLC system for estradiol analysis without any pre-treatment.

2.6.5.2. RP- HPLC fluorescence analysis of estradiol. An HPLC method was developed and validated for estradiol assay in rat plasma samples. The HPLC equipment consisted of a HITACHI L-7110 Intelligent HPLC pump, and a HITACHI L-7200 Intelligent HPLC Autosampler, a HITACHI FL Detector L-7485 set at 267 nm (λ_{ex}) and 302 nm (λ_{em}), and a ANASTAR Chromatography Data System. Separation was achieved at 30 °C on a Kromasil C_{18} column (200 mm × 4.6 mm, particle size 5 μm, Zirchrom company). The mobile phase consisted of acetonitrile–water (40:60 for plasma samples, and 50:50 for CSF samples), filtered and degassed under reduced pressure, prior to use. A guard column was used to prevent column clogging. The flow rate was 1.0 ml min^{-1}.

2.6.6. Data analysis

Absolute concentrations in CSF were calculated from the concentrations in the dialysates using the following equation: $C = C_d/R$, where R is the in vivo relative recovery. The area under the plasma concentration–time curve AUC_{plasma} value and CSF concentration–time curve AUC_{CSF} value were calculated using the trapezoidal rule.

The degree of E_2 targeting to CSF after intranasal administration can be evaluated by the drug targeting index (DTI) [21,22], which can be described as the ratio of the value of AUC_{CSF}/AUC_{plasma} following intranasal administration to that following intravenous injection. The higher the DTI is, the further degree of E_2targeting to CSF can be expected after intranasal administration.

$$\mathrm{DTI} = \frac{(\mathrm{AUC}_{\text{brain tissue}}/\mathrm{AUC}_{\text{plasma}})_{\text{i.n.}}}{(\mathrm{AUC}_{\text{brain tissue}}/\mathrm{AUC}_{\text{plasma}})_{\text{i.v.}}} \quad (3)$$

In order to more clearly understand the direct transfer of E_2 between nose and brain after i.n. administration, drug targeting percentage (DTP) [23] was introduced, the equations are as follows:

$$\mathrm{Bx} = (\mathrm{B_{iv}}/\mathrm{P_{iv}}) \times \mathrm{P_{in}} \quad (4)$$

$$DTP\% = \frac{B_{i.n.} - B_x}{B_{i.n.}} \times 100\% \quad (5)$$

where, $Bx = AUC_{CSF}$ fraction contributed by systemic circulation through the blood–brain barrier (BBB) following intranasal delivery, $B_{i.v.} = AUC_{CSF}$ following intravenous administration, $P_{i.v.} = AUC_{plasma}$ after intravenous administration, $B_{i.n.} = AUC_{CSF}$ flowing intranasal delivery, $P_{i.n.} = AUC_{plasma}$ by intranasal administration.

Statistical differences between i.n. and i.v. administration were concluded using the unpaired Student's t-test and a value of $P < 0.05$ was considered statistically significant. Results were presented as mean values ± SD.

3. Results

3.1. Particle size and zeta potential of E_2 CS-NPs

As mentioned above, chitosan particles are formed by the ionic crosslinking (ionotropic gelation) between oppositely charged ions

[24,25]. The production process of nanoparticles is dependent on the number of positively charged groups left on the dissolved chitosan molecules. Because of enough protonated amine groups remaining, the process of the ionic crosslinking occurs more easily for chitosan with high degree of deacetylation. The data of mean particle size and zeta potential are listed in Table 1.

Besides chitosan with Mw 50,000, chitosans with M_w 6000 and 200,000 were also studied. However, the particle size was too small (below 100 nm) or too large (above 500 nm), and finally, chitosan with M_w 50,000 was chosen to prepare CS-NPs to obtain particle size about 260 nm.

Nicomp distribution was adopted for the determination of particle size and distribution of CS-NPs, science chi square was too large for Gaussian distribution, meaning Gaussian distribution was not accurate enough. In each diagram of the Nicomp distribution, there was a smaller peak in the particle size range of 50–100 nm, which demonstrated that maybe chitosan with much smaller molecular weight existed.

The surface charge is the critical parameter on the stability of suspensions and adhesion of particle systems onto biological surfaces. Consequently, investigation of zeta potential is an important part of nanoparticle characterization. Chitosan nanoparticles are all positively charged which is a typical characteristic of chitosan/TPP particles. This can be explained by the particle formation mechanism, the positively charged amine groups are neutralized by their interaction with the negative charge in tripolyphosphate molecules [26]. The residual amino groups would be responsible for the positive potential.

The higher zeta potential in a certain range implies that chitosan nanoparticles are more stable. It seems likely that the long amino groups hinder the anion adsorption and keep the high value of the electrical double layer thickness, suggesting the prevention of aggregation. The zeta potentials in three batches of CS-NPs are over +20 mv.

3.2. Loading capacity and entrapment efficiency of E_2 CS-NPs

The loading capacity and entrapment efficiency of CS-NPs are shown in Table 2.

3.3. Pharmacokinetic study

Analytical method used in pharmacokinetic study followed the in vivo method reported before [16]. The calculated concentrations of estradiol in blood after intranasal and intravenous administration are shown in Fig. 3.

For intravenous delivery, the C_{max} (151.4 ± 28.2 ng ml^{-1}) are reached at the first beginning (Fig. 3), and then followed by an exponential decline depending on the time. Comparatively, nasally applied E_2 displayed a slow and poor absorption across the nasal mucosa into the systemic circulation, 28 min after nasal administration, E_2 plasma concentration reached a peak value of (32.7 ± 10.1) ng ml^{-1}, far lower than the maximal plasma concentration of i.v. injected E_2.

Table 1
The particle size and ξ-potential test results of the three batches of E_2 CS-NPs

Batch	Nicomp distribution			ξ-Potential (mV)
	Peak number	Particle size (nm)	SD (nm)	
20050919	Peak 1	86.2 (9.6%)	8.4	+25.4
	Peak 2	273.9 (90.4%)	27.9	
20050920	Peak 1	60.8 (8.8%)	6.4	+24.8
	Peak 2	268.1 (91.2%)	33.4	
20050921	Peak 1	86.0 (13.4%)	9.6	+26.2
	Peak 2	265.8 (86.6%)	33.5	

Table 2
The loading capacity and encapsulation efficiency of the three batches of E_2 CS-NPs

Batches	20050919	20050920	20050921
LC (mg ml^{-1})	1.9	1.9	2.0
EE (%)	63.2	66.4	64.6

Selected pharmacokinetic parameters by intranasal and intravenous administration calculated from the individual time-concentration profiles from the experiment are shown in Table 3, where values of AUC, C_{max}, absorption rate, half-life and T_{max} can be found.

Significant differences between intranasal and intravenous delivery were found (t-test) for the calculated pharmacokinetic parameters, except for K_e, $t_{1/2}$, MRT.

Obviously, for E_2 CS-NPs, the concentrations of E_2 in the blood were quite different after intranasal and intravenous delivery, only small amount of E_2 was absorbed into the blood circulation.

3.4. Brain-targeting study

To determine whether or not estradiol is transported from the nasal cavity into the CSF via the olfactory neurons, estradiol was administered intranasally and intravenously in the same set of rats. In vitro recovery of microdialysis probe and in vivo recovery were necessary for calculating E_2 concentration in CSF, which were published before [16].

The calculated concentrations of estradiol in CSF after intranasal and intravenous administration are shown in Fig. 4, and the important parameters are listed in Table 4.

It was found that the E_2 levels in CSF of nasal route were significantly higher than those obtained after i.v. injection despite the much lower E_2 concentrations in plasma of nasal route than those of i.v. injection. In CSF, estradiol had a C_{max} of (76.4 ± 14.0) ng ml^{-1} (Fig. 4) at 28 min after intranasal delivery, but delayed to 60 min (29.5 ± 7.4 ng ml^{-1}) (Fig. 4) by intravenous administration, which illustrated that E_2 could arrive at the brain tissue earlier following intranasal administration.

As seen in Table 5, DTI was 3.2, greater than 1, and DTP was 68.4%, we can observe a measurable degree of E_2 targeting to CSF following intranasal administration.

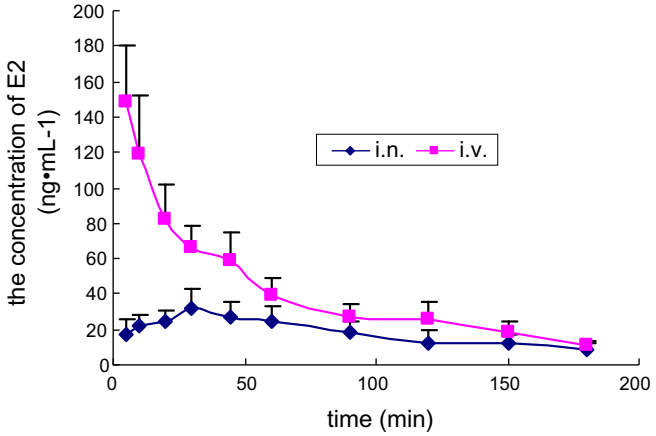

Fig. 3. The mean plasma concentration–time curves of estradiol in rats after intranasal and intravenous administration of estradiol CS-NPs at the dose of 0.48 mg kg^{-1}. (n = 5, mean ± SD).

Table 3
Pharamacokinetic parameters of estradiol CS-NPs after intranasal and intravenous administration to rats at the dose of 0.48 mg kg^{-1} in plasma (n = 5, mean ± SD)

Adminis tration	C_{max} ($\times 10^2$ ng·ml^{-1})	T_{max} ($\times$10 min)	Ke ($\times 10^{-1}$ min^{-1})	$t_{1/2}$ ($\times$10 min)	$AUC_{0-\infty}$ ($\times 10^3$ ng min ml^{-1})	$AUMC_{0-\infty}$ ($\times 10^5$ ng min ml^{-1})	MRT ($\times 10^2$ min)
i.n.	0.33 ± 0.10	2.8 ± 0.45	0.08 ± 0.02	9.43 ± 2.06	6.06 ± 2.38	6.39 ± 2.87	1.03 ± 0.14
i.v.	1.51 ± 0.28		0.09 ± 0.03	8.64 ± 3.40	9.18 ± 2.63	8.98 ± 3.07	0.98 ± 0.21

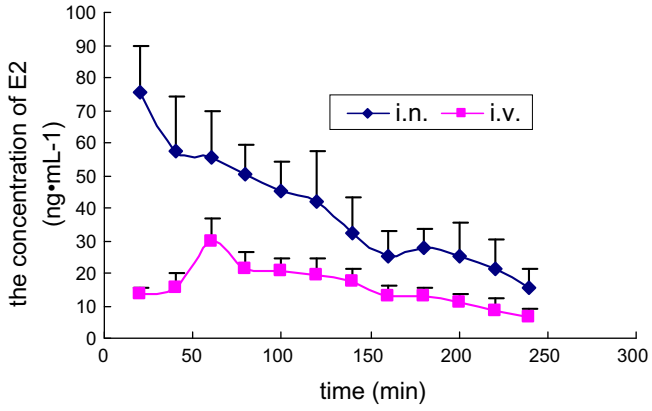

Fig. 4. The mean CSF concentration–time curves of estradiol in rats after intranasal and intravenous administration of estradiol CS-NPs at the dose of 0.48 mg kg^{-1} (n = 5, mean ± SD).

4. Discussion

However, the nasal cavity only has a total volume of 15–20 ml and a total surface area of about 150 cm^2, therefore, volume that can be delivered into the nasal cavity is restricted to 25–200 μl, therefore, in order to increase E_2 solubility in water, E_2 inclusion complex was prepared, and then made into CS-NPs.

The preparation of CS nanoparticles, based on an ionic gelation process, involves the mixture of two aqueous phases at room temperature. One phase contains a solution of CS and the other contains a solution of the polyanion TPP, the reaction between CS and TPP is shown in Fig. 5.

Chitosan has many advantages, particularly for developing nanoparticles. These include: its ability to control the release of active agents, it avoids the use of hazardous organic solvents while fabricating particles since it is soluble in aqueous acidic solution, it is a linear polyamine containing a number of free amine groups that are readily available for crosslinking, its cationic nature allows for the ionic crosslinking with multivalent anions, it has mucoadhesive character, which increases residual time at the site of absorption, and so on. LD_{50} of CS in laboratory mice is 16 g kg^{-1} body weight, which is close to sugar or salt. Chitosan is proven to be safe in rats up 10% in the diet [27,28].

Microdialysis was originally developed to measure the concentrations of endogenous substances in the extracellular fluid (ECF) of normal brain [29], particularly neurotransmitters [30], and it has since become an important tool to investigate the disposition of many classes of drugs [31].

The concentrations of the drug in the dialysate reflect the concentrations in the (extracellular) fluid around the semipermeable part of the probe. However, as the dialysis procedure is not performed under equilibrium conditions, the concentration in the

Table 4
Pharmacokinetic parameters of estradiol CS-NPs after intranasal and intravenous administration to rats at the dose of 0.48 mg kg^{-1} in CSF (n = 5, mean ± SD)

Rat	i.n.			i.v.		
	C_{max} (ng ml^{-1})	T_{max} (min)	$AUC_{0-\infty}$ (ng min ml^{-1})	C_{max} (ng ml^{-1})	T_{max} (min)	$AUC_{0-\infty}$ (ng min ml^{-1})
Mean	76.4	28	12788.4	29.5	60	6121.0
SD	14.0	17.9	4093.6	7.4	0	2075.9

Table 5
DTI and DTP of E_2 CS-NPs by intranasal administration (mean ± SD, n = 5)

Administration	AUC_{CSF} (ng min ml^{-1})	AUC_{plasma} (ng min ml^{-1})	AUC_{CSF}/AUC_{plasma}	DTI	DTP (%)
i.n.	12788.4 ± 4093.6	6057.1 ± 2385.0	2.1 ± 1.7	3.2	68.4
i.v.	6121.0 ± 2075.9	9183.9 ± 2631.1	0.7 ± 0.8		

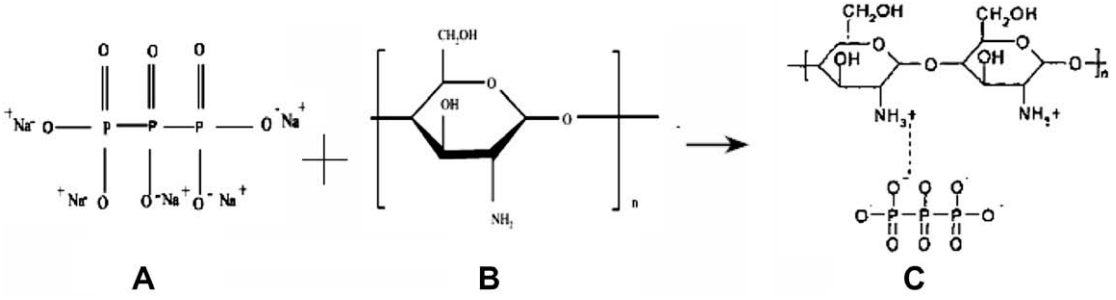

Fig. 5. The formation of chitosan nanoparticle by ionic gelation process. (A) Sodium tripolyphosphate, (B) chitosan, (C) chitosan nanoparticle.

dialysate will be different from that in the periprobe fluid. The term recovery is used to describe this relationship. As we reported before [16], in vivo recovery (41.7%) was much lower than in vitro recovery of the probe (61.6%).

It is well known that the euphoria derived from the sniffing of cocaine in conscious subjects occurs rapidly (within 3–5 min). It has been suggested that the reason for such rapid effects is, apart from a rapid nasal absorption, the presence of a direct pathway from the nasal cavity to the CNS and the capacity of the drug to concentrate selectively in specific regions in the brain. Various studies in animal models have confirmed that, at early time points after nasal administration, the concentration of cocaine in the brain was higher after nasal administration than after intravenous injection, thereby showing the existence of the pathway from nose to brain [32,33].

Similar result had been found for estradiol in our former experiment [16], which was also testified in this study. Compared to E_2 inclusion complex (see [16], Fig. 7), E_2 CS-NPs gained higher E_2 concentration in CSF at each sampling time following intranasal delivery, resulting in higher AUC_{CSF} value, which proved that CS-NPs are a more suitable formulation for E_2 to be transported into CNS.

It can be explained as follows: CS-NPs can bind strongly to negatively charged materials such as cell surfaces and mucus. Mucus contains mucins that have different chemical constitutions, but some contain significant proportions of sialic acid. At physiological pH, sialic acid carries a net negative charge and, as a consequence, mucin and chitosan can demonstrate strong electrostatic interaction in solution. It is evident that chitosan behaves as a bioadhesive material increasing significantly the half-time of clearance [34–36].

However, the absorption promoting effect of chitosan is due not only to improved adhesion between the formulation and the nasal tissues, but also to a transient effect of chitosan on paracellular transport processes. Investigations in cell culture (CaCo-2) as well as in animal models have demonstrated that chitosan can have an effect in modifying paracellular transport [37]. Immunohistological studies have shown that chitosan can open the tight junctions between cells through an effect upon Factin filaments. Unlike other absorption promoters, chitosan appears to be non-toxic and well tolerated by human subjects. This combination of bioadhesion and paracellular transport effects has led to a consideration of the use of chitosan for the delivery of E_2 via the nasal cavity.

References

[1] M.P. Daly, Diagnosis and management of Alzheimer disease, J. Am. Board Fam. Pract. 12 (1999) 375–385.
[2] H. Kölsch, M.L. Rao, Neuroprotective effects of estradiol-17β: implications for psychiatric disorders, Arch. Womens Ment. Health 5 (2002) 105–110.
[3] J. Nilsen, R.W. Irwin, T.K. Gallaher, et al., Estradiol in vivo regulation of brain mitochondrial proteome, J. Neurosci. 27 (2007) 14069–14077.
[4] Related articles, N. LinksSchupf, S. Winsten, B. Patel, et al., Bioavailable estradiol and age at onset of Alzheimer's disease in postmenopausal women with down syndrome, Neurosci. Lett. 406 (2006) 298–302.
[5] L. Illum, Transport of drugs from the nasal cavity to the central nervous system, Eur. J. Pharm. Sci. 11 (2000) 1–18.
[6] S. Mathison, R. Nagilla, U.B. Kompella, Nasal route for direct delivery of solutes to the central nervous system: fact or fiction?, J Drug Target. 5 (1998) 415–441.
[7] W. Ulrika, P. Elena, J. Björn, et al., Transfer of morphine along the olfactory pathway to the central nervous system after nasal administration to rodents, Eur. J. Pharm. Sci. 24 (2005) 565–573.
[8] R.G. Thorne, G.J. Pronk, V. Padmanabhan, et al., Delivery of insulin-like growth factor-I to the rat brain and spinal cord along olfactory and trigeminal pathways following intranasal administration, Neuroscience 127 (2004) 481–496.
[9] H. Critchley, S.S. Davis, N.F. Farraj, et al., Nasal absorption of desmopressin in rats and sheep. Effect of a bioadhesive microsphere delivery system, J. Pharm. Pharmacol. 46 (1994) 651–656.
[10] L. Illum, N. Farraj, H. Critchley, et al., Nasal administration of gentamicin using a novel microsphere delivery system, Int. J. Pharm. 46 (1988) 261–265.
[11] E. Bjork, P. Edman, Characterization of degradable starch microspheres as a nasal delivery system for drugs, Int. J. Pharm. 62 (1990) 187–192.
[12] P. Dondeti, H. Zia, T.E. Needham, Bioadhesive and formulation parameters affecting nasal absorption, Int. J. Pharm. 127 (1996) 115–133.
[13] Q. Li, T. Dunn, E.W. Grandmaison, M.F.A. Goodsen, Applications and properties of chitosan, J. Bioact. Compatible Polym. 7 (1992) 370–397.
[14] H.K. Alexander, G. Davide, B.S. Andreas, Thiolated chitosan microparticles: a vehicle for nasal peptide drug delivery, Int. J. Pharm. 307 (2006) 270–277.
[15] L. Ilium, N.F. Farraj, S.S. Davis, Chitosan as a novel nasal delivery system for peptide drugs, Pharm. Res. 11 (1994) 1186–1189.
[16] Xiaomei Wang, Haibing He, Wei Leng, et al., Evaluation of brain-targeting for the nasal delivery of estradiol by the microdialysis method, Int. J. Pharm. 317 (2006) 40–46.
[17] H. Komatsu, A. Kitajima, S. Okada, Pharmaceutical characterization of commercially available intravenous fat emulsions: estimation of average particle size, size distribution and surface potential using photon correlation spectroscopy, Chem. Pharm. Bull. 43 (1995) 1412–1415.
[18] Wei Leng, Wanping Ding, Xing Tang, Studies of estradiol-methyl-β-cyclodextrin complexes nasal absorption kinetics, J. Shenyang Pharm. Univ. 22 (2005) 171–175.
[19] S. Hirai, T. Yashiki, T. Matsuzawa, H. Mima, Absorption of drugs from the nasal mucosa, Int. J. Pharm. 7 (1981) 317–325.
[20] C.H. Huang, R. Kimura, R. Bawarshi-Nassar, A. Hussain, Mechanism of nasal absorption of drugs I: physicochemical parameters influencing the rate of in situ nasal absorption of drugs in rats, J. Pharm. Sci. 74 (1985) 608–611.
[21] T. Sakane, S. Yamashita, N. Yata, et al., Transnasal delivery of 5-fluorouracil to the brain in the rat, J. Drug Target. 7 (1999) 233–240.
[22] F. Wang, X. Jiang, W. Lu, Profiles of methotrexate in blood and CSF following intranasal and intravenous administration to rats, Int. J. Pharm. 263 (2003) 1–7.
[23] Q. Zhang, X. Jiang, W. Jiang, W. Lu, L. Su, Z. Shi, Preparation of nimodipine-loaded microemulsion for intranasal delivery and evaluation of the targeting efficiency to brain, Int. J. Pharm. 275 (2004) 85–96.
[24] P. Calvo, C. Remunan-Lopez, J.L. Vila-Jato, M.J. Alonso, Novel hydrophilic chitosan-polyethylene oxide nanoparticles as protein carriers, J. Appl. Polym. Sci. 63 (1997) 125–132.
[25] C. Remunan-Lopez, R. Bodmeier, Effect of formulation and process variables on the formation of chitosan-gelatin coacervatives, Int. J. Pharm. 135 (1996) 63–72.
[26] R. Fernandez-Urrusuno, D. Romani, P. Calvo, et al., Development of a freeze-dried formulation of insulin-loaded chitosan nanoparticles intended for nasal administration, STP Pharm. Sci. 5 (1999) 429–436.
[27] K. Arai, T. Kinumaki, T. Fujita, Toxicity of chitosan, Bull. Tokai Reg. Fish Lab. 43 (1968) 89–94.
[28] W. Paul, C.P. Garside, Chitosan, a drug carrier for the 21st century: a review, STP Pharm. Sci. 10 (2000) 5–22.
[29] L. Bito, H. Davson, E. Levin, M. Murray, N. Snider, The concentrations of free amino acids and other electrolytes in cerebrospinal fluid, in vivo dialysate of brain, and blood plasma of the dog, J. Neurochem. 13 (1966) 1057–1067.
[30] B.H. Westerink, Brain microdialysis and its application for the study of animal behaviour, Behav. Brain Res. 70 (1995) 103–124.
[31] W.F. Elmquist, R.J. Sawchuk, Application of microdialysis in pharmacokinetic studies, Pharm. Res. 14 (1997) 267–288.
[32] L. Illum, Transport of drugs from the nasal cavity to the central nervous system, Eur. J. Pharm. Sci. 11 (2000) 1–18.
[33] H. Chow et al., Direct transport of cocaine from the nasal cavity to the brain following intranasal cocaine administration in rats, J. Pharm. Sci. 88 (1999) 754–758.
[34] R.J. Soane, M. Frier, A.C. Perkins, et al., Evaluation of the clearance characteristics of bioadhesive systems in humans, Int. J. Pharm. 178 (1999) 55–65.
[35] P. Artursson, T. Lindmark, S.S. Daris, et al., Effect of chitosan on the permeability of monolayers of intestinal epithelial cells (Caco-2), Pharm. Res. 11 (1994) 1358–1361.
[36] H.L. Luessen, B.J. De Leeuw, M. Langemeyer, et al., Mucoadhesive polymers in peroral peptide drug delivery. IV. Carbomer and chitosan improve the intestinal absorption of the peptide drug buserelin in vivo, Pharm. Res. 13 (1996) 1668–1672.
[37] V. Dodane, M.A. Khan, J.R. Merwin, Effect of chitosan on epithelial permeability and structure, Int. J. Pharm. 182 (1999) 21–32.